Spectroscopic Comparisons of MoW(porphyrin)$_2$ Heterodimers with Homologous Mo_2 and W_2 Quadruple Bonds: A Dynamic NMR and Resonance Raman Study

James P. Collman,*,† S. T. Harford,† Stefan Franzen,‡,§ T. A. Eberspacher,† Richard K. Shoemaker,⊥ and William H. Woodruff‡

Contribution from the Department of Chemistry, Stanford University, Stanford, California 94305, Los Alamos National Laboratory, Los Alamos, New Mexico 87545, and University of Nebraska−Lincoln, Lincoln, Nebraska 68588

Received June 26, 1997

Abstract: The rotational barrier for MoW(*meso*-monotolyl octaethylporphyrin)$_2$ ([(TOEP)MoW(TOEP)]) has been determined ($\Delta G^{\ddagger}_{rot} = 10.6 \pm 0.1$ kcal/mol) by variable-temperature NMR and complete band shape analysis and is compared with values previously obtained for the analogous homodimers. The overall quadruple bond strengths of these isostructural dimolybdenum, ditungsten, and molybdenum−tungsten porphyrin dimers have also been compared by calculation of the force constants corresponding to each metal−metal bond stretching frequency as observed by resonance Raman spectroscopy. The Raman results are as follows: [Mo(OEP)]$_2$, $\nu_{MoMo} = 310$ cm^{-1}, $k = 2.72$ mdyn/Å; [(OEP)MoW(OEP)], $\nu_{MoW} = 279$ cm^{-1}, $k = 2.89$ mdyn/Å; [Mo(TOEP)]$_2$, $\nu_{MoMo} = 310$ cm^{-1}, $k = 2.72$ ν_{MoMo} [W(TOEP)]$_2$, $\nu_{WW} = 275$ cm^{-1}, $k = 4.08$ mdyn/Å; and [(TOEP)MoW(TOEP)], $\nu_{MoW} = 278$ cm^{-1}, $k = 2.87$ mdyn/Å. Both the ^{1}H NMR and Raman specta are consistent with a [(Por)MoW(Por)] structure wherein the Mo(Por) congener experiences a more drastic "bending-back" distortion of the porphyrin macrocycle.

Introduction

The first reported heteronuclear quadruple bonds between molybdenum and tungsten appeared to be some of the strongest bonds found in coordination complexes.[1] Cotton et al. have reported that the compound MoW(mhp)$_4$ (mhp = 2-hydroxy-6-methylpyridine anion) exhibits a larger force constant for the metal−metal stretch and a formally shorter bond length than either of the corresponding homodimers.[2] McCarley's laboratory has also found a shorter bond in the MoW(O$_2$CCMe$_3$)$_4$ dimer relative to its homonuclear analogues.[3] These observations led to a proposition that polar, heteronuclear metal−metal bonds exhibit a "special stability" relative to the homonuclear congeners.

More recently, the independent syntheses of MoWCl$_4$(PR$_3$)$_4$ (PR$_3$ = PMePh$_2$, PMe$_2$Ph, or PMe$_3$) by Morris[4] and McCarley[5] provided the first family of unbridged molybdenum−tungsten quadruple bonds. The preliminary information available from electronic absorption spectroscopy,[4] cyclic voltammetry,[4] X-ray crystallography,[3,6] photoelectron spectroscopy,[7] and resonance Raman[7] studies of these molecules suggests that the unbridged heteronuclear dimers exhibit properties which are the *average* of the homonuclear dimers. Evaluation of the apparently deviant properties of bridged heteronuclear dimers became the subject of a review by Morris,[8] in which the "enhanced stability" of bridged heterodimers was attributed to ligand steric preferences.

We have recently developed a single-step preparation of the heterometallic porphyrin dimer [(OEP)MoW(OEP)] (**1**) containing an unsupported quadruple bond between molybdenum and tungsten. We report here the relative bond strengths for homologous dimolybdenum, ditungsten, and molybdenum−tungsten porphyrin dimers. The novel heterodimer [(TOEP)MoW(TOEP)] (**2**) (TOEP = *meso*-(4′-tolyl)octaethylporphyrin) has been synthesized to calculate the barrier to rotation about the mixed-metal δ-bond. Rotational barriers for [Mo(TOEP)]$_2$ (**3**) and [W(TOEP)]$_2$ (**4**) have been previously reported.[9]

Vibrational spectroscopy has been employed to determine ν_{MM}, and the corresponding force constants have been calculated for these same group VIB dimers. With these techniques a single component of the metal−metal quadruple bond as well as the overall multiple metal−metal bond may both be directly studied for evidence of an enhanced stability in the heteronuclear species.

† Stanford University.
‡ Los Alamos National Laboratory.
§ Current address: North Carolina State University, Raleigh, NC 27695.
⊥ University of Nebraska−Lincoln.

(1) (a) Bursten, B. E.; Cotton, F. A.; Cowley, A. H.; Hanson, B. E.; Lattman, M.; Stanley, G. G. *J. Am. Chem. Soc.* **1979**, *101*, 6244. (b) Cotton, F. A.; Hanson, B. E. *Inorg Chem.* **1978**, *17*, 3237.
(2) (a) Katovic, V.; Templeton, J. L.; Hoxmeier, R. J.; McCarley, R. E. *J. Am. Chem. Soc.* **1975**, *97*, 5300. (b) Katovic, V.; McCarley, R. E. *J. Am. Chem. Soc.* **1978**, *100*, 5586.
(3) Luck, R. L.; Morris, R. H. *J. Am. Chem. Soc.* **1984**, *106*, 7978.
(4) Carlin, R. T. Ph.D. Thesis, Iowa State University, 1982.
(5) (a) Luck, R. L.; Morris, R. H.; Sawyer, J. F. *Inorg. Chem.* **1987**, *26*, 2422.
(6) Bancroft, G. M.; Bice, Jo-Ann; Morris, R. H.; Luck, R. L. *J. Chem. Soc., Chem. Commun.* **1986**, 898.
(7) Carlin, R. T.; McCarley, R. E. *Inorg. Chem.* **1989**, *28*, 280.
(8) Morris, R. H. *Polyhedron* **1987**, *6*, 793.
(9) Collman, J. P.; Garner, J. M.; Hembre, R. T.; Ha, Y. *J. Am. Chem. Soc.* **1992**, *114*, 1292.

S0002-7863(97)02130-6 CCC: $15.00
Published on Web 02/06/1998

Experimental Section

Materials. H_2OEP and H_2TOEP were synthesized simultaneously by an adaptation[10] of the published procedure for H_2OEP.[11] Diethylpyrrole was donated by Pharmacyclics and distilled immediately prior to use. $Mo(CO)_6$ and $W(CO)_6$, cobaltocene, and ferricinium hexafluorophosphate were purchased from Strem and used as received. Benzene-d_6 and toluene-d_8 were purchased from Cambridge Isotope Laboratories and vacuum distilled from sodium−benzophenone ketyl immediately prior to use. Solvents used for the metalation (Decalin) and manipulation (benzene) of the dimers were distilled from sodium benzophenone ketyl under argon before introduction into the glovebox. $[Mo(OEP)]_2$,[12] $[W(OEP)]_2$,[13] $[Mo(TOEP)]_2$,[10] and $[W(TOEP)]_2$[10] were prepared according to published procedures.

Physical Measurements. A nitrogen-filled Vacuum Atmospheres drybox equipped with a Dri-Train inert gas purifier was employed for manipulations carried out under anaerobic conditions. ^{1}H NMR spectra were recorded on a Varian XL-400 or General Electric 500 Omega FT-NMR spectrometer using benzene-d_6 or toluene-d_8 as a solvent. Resonances in the ^{1}H NMR were referenced versus the residual proton signal of the solvent. The mixing time for the 2D NOESY/EXCHSY spectra was 100 ms. Resonance Raman samples were prepared in the glovebox and flame sealed under vacuum.

Excitation for the RR experiments was provided by an Ar^+ ion laser (Spectra Physics Model 171). Typical laser powers were 20−30 mW on resonance. Scattered light was collected by an f/1 5 cm focal length lens and focused onto the slit of a SPEX 0.6 operating as a spectrograph to disperse the light onto a Photometrics CCD camera. Typical data acquisition times were 20 min. Because the precision of the depolarization ratios (ρ) was ±0.1, only general information such as whether bands were polarized (a_{1g} modes), depolarized (b_{1g} and b_{2g}), or anomalously polarized (a_{2g}) could be determined.

Mass spectrometry was performed at the Mass Spectrometry Facility at the University of California−San Francisco and by Dr. Doris Hung of the Analytical Services Division at Northwestern University.

Preparation of 5-(4′-Methylphenyl)-2,3,7,8,12,13,17,18-octaethylporphyrin, H_2TOEP.[11] A 3000 mL, three-neck, round-bottom flask was wrapped in aluminum foil and equipped with a Dean−Stark trap, stir bar, and argon inlet. The flask was charged with 3,4-diethylpyrrole (5.00 g, 40.6 mmol) and 1500 mL of benzene and was sparged with nitrogen for 25 min. To this were added *p*-tolualdehyde (1.44 mL, 12.2 mmol), aqueous formaldehyde (2.76 mL of 37% solution, 34.7 mmol), and *p*-toluenesulfonic acid (150 mg, 0.79 mmol). The mixture was stirred at 100 °C for 8 h. The reaction mixture was allowed to cool, and the solution was bubbled with O_2 for 12 h. The mixture was concentrated under vacuum and the residue redissolved in chloroform (300 mL). The resulting solution was washed once with 1 N aqueous NaOH (200 mL) and twice with water (100 mL) and then concentrated in vacuo. The crude reaction mixture was chromatographed with CH_2Cl_2 on a plug of alumina (15 cm × 5 cm) to remove polymeric impurities. A second column was run using flash silica and CH_2Cl_2 to remove bulk H_2OEP (major product). H_2TOEP was eluted from the silica using a 5% ethyl acetate in CH_2Cl_2 system. The H_2TOEP was chromatographed a third time using conditions identical to those of the second chromatography to remove any trace impurities; this yielded 368 mg (0.589 mmol, 5.8% yield) of H_2TOEP. ^{1}H NMR (C_6D_6): δ 10.43 (s, 2H, H_{cis}), 10.17 (s, 1H, H_{trans}), 4.31 (m, 12H, $-CH_2CH_3$), 3.05 (q, 4H, $-CH_2CH_3$), 2.15 (t, 18H, $-CH_2CH_3$), 1.42 (t, 6H, $-CH_2CH_3$), 8.31 (d, 2H, H_o), 7.65 (d, 2H, H_m), 2.89 (s, 3H, aryl-CH_3), −2.72 (s, 1H, N*H*), −2.81 (s, 1H, N*H*). Mass spectrum: *m*/*e* calcd 625.5, found 625.5.

Preparation of [(OEP)MoW(OEP)] (1). In the glovebox, a 100 mL round-bottom flask equipped with a Teflon vacuum valve and no. 9 O-ring sidearm was charged with 10 mL of Decalin, H_2OEP (250 mg, 0.468 mmol), $W(CO)_6$ (800 mg, 2.27 mmol), $Mo(CO)_6$ (100 mg, 0.379 mmol), and a stir bar. The headspace was evacuated at 10^{-2} Torr for 10−15 min to remove adventitious oxygen and water. The sealed flask was heated at 180 °C for 6 h, cooled to ambient temperature, and transferred to the glovebox and held at −20 °C overnight. (*Caution!* Although heating a closed system in this manner may often be hazardous and ill-advised, at this temperature the vapor pressure of Decalin is still less than 1 atm and the reaction is at a slightly negative pressure.) The mixture of [(OEP)MoW(OEP)] (**1**) (82 mg, 13.7%), $[Mo(OEP)]_2$ (**5**) (197 mg, 34.1%), and $[W(OEP)]_2$ (**6**) (25 mg, 4.5%) was collected by filtration and washed with cold hexane. The ditungsten species, **6**, was removed as the monocation (EPR $g_{av} = 1.87$) by titration of a benzene solution of the three dimers with a stoichiometric amount (5.80 mg, 0.0175 mmol) of ferricinium hexafluorophosphate (as determined by integration of H_{meso} resonances in the ^{1}H NMR and total mass of the mixture) followed by filtration and washing of the collected solid with benzene. $[(OEP)MoW(OEP)]^+PF_6^-$ (**7**) was then isolated by a second titration with ferricinium hexafluorophosphate (16.1 mg, 0.0487 mmol) and collected by filtration and washed with benzene. The yield was 73 mg (9.8% based on porphyrin). EPR (frozen CH_2Cl_2): $g_\perp = 1.89$, $g_\perp = 1.94$. Mass spectrum: *m*/*e* $(OEP)MoW(OEP)^+$ (cluster) calcd 1344.6, found 1345 (see the Supporting Information).

7 (12 mg, 8.06 mmol) was suspended in 5 mL of stirring benzene, and a stock solution of cobaltocene (5 mg, 26.4 mmol in 2 mL of benzene) was slowly added dropwise. The solution immediately darkened and was allowed to stir for 2 h. The solution was filtered to remove insoluble cobaltocinium hexafluorophosphate and the solvent removed in vacuo. Unreacted cobaltocene was removed by sublimation. The product was dried at 50 °C and 10^{-2} Torr for 4 h. The yield was 10 mg, (95%). UV−vis (nm) (log ϵ, C_6H_6): Soret 382 (4.86), 435 (4.56), 532 (3.50), 560 (3.66). ^{1}H NMR (ppm, C_6D_6): δ 9.06 (s, 4H, Mo H_{meso}); 8.68 (s, 4H, W H_{meso}); 4.22−4.35 (m, 8H, $J = 7.6$ Hz, Mo $-CH_2CH_3$), 3.82−3.95 (m, 8H, $J = 7.6$ Hz, Mo $-CH_2CH_3$); 4.15−4.27 (m, 8H, $J = 7.4$ Hz, W $-CH_2CH_3$), 3.75−3.87 (m, 8H, $J = 7.4$ Hz, W $-CH_2CH_3$); 1.74 (t, 24H, $J = 7.6$ Hz, Mo $-CH_2CH_3$); 1.72 (t, 24H, $J = 7.4$ Hz, W $-CH_2CH_3$). Mass spectrum *m*/*e* (cluster) calcd 1344.6, found 1345.

Preparation of [(TOEP)MoW(TOEP)] (2). The procedure was identical to that used for the synthesis of **1**. A 75 mg (0.120 mmol) sample of H_2TOEP yielded 10 mg (0.0065 mmol) of [(TOEP)MoW(TOEP)] (overall yield is 5.5%, based on porphyrin). UV−vis nm (log ϵ, C_6H_6): Soret 384 (4.82), 437 (4.49), 537 (3.56), 566 (3.59). ^{1}H NMR (ppm, C_6D_6): δ 9.19 (s, 2H, Mo H_{cis}), 9.41 (s, 1H, Mo H_{trans}), 4.25−4.50 (m, 6H, Mo $-CH_2CH_3$), 3.00−3.10 (q, 2H, Mo $-CH_2CH_3$), 3.73−3.99 (m, 6H, Mo $-CH_2CH_3$), 2.75−2.86 (q, 2H, Mo $-CH_2CH_3$), 1.65 (t, 18H, Mo $-CH_2CH_3$), 1.39 (t, 6H, $-CH_2CH_3$), 9.91 (d, 1H, Mo $H_{o'}$), 7.95 (d, 1H, Mo $H_{m'}$), 6.98 (d, 1H, Mo H_o), 6.98 (d, 1H, Mo H_m), 8.81 (s, 2H, W H_{cis}), 8.97 (s, 1H, W H_{trans}), 4.13−4.35 (m, 6H, W $-CH_2CH_3$), 2.91−3.00 (q, 2H, W $-CH_2CH_3$), 3.61−3.85 (m, 6H, W $-CH_2CH_3$), 2.65−2.74 (m, 2H, W $-CH_2CH_3$), 1.62 (t, 18H, W $-CH_2CH_3$), 1.36 (t, 6H, W $-CH_2CH_3$), 9.86 (d, 1H, W $H_{o'}$), 7.95 (d, 1H, W $H_{m'}$), 6.98 (d, 1H, W H_o), 6.98 (d, 1H, W H_m), 2.59 (s, 3H, aryl-CH_3). Mass spectrum: *m*/*e* (cluster) calcd = 1526.6, found 1527 (see the Supporting Information).

Results

^{1}H NMR: Rapid Rotation Regime. To be consistent with our previous study[9] of the rotational barriers for **3** and **4**, we employed a single *meso*-tolyl substituent to break the characteristic 4-fold symmetry of octaethylporphyrin and divide the remaining *meso*-protons into two which are adjacent to the tolyl substituent, H_{cis}, and one which is opposed, H_{trans}. The chemical shift difference between these *meso*-protons results from through-bond[14] and through-space contributions from the *meso*-tolyl substitutent. A characteristic 2:1 set of *meso*-proton

(10) Dr. Hilary Arnold Godwin, now an Associate Professor of Chemistry at Northwestern University, first applied the Sessler et al. H_2OEP preparation to synthesis of *meso*-substituted H_2OEP derivatives. See: Godwin, H. A. Ph.D. Thesis, Stanford University, 1994.

(11) Sessler, J. L.; Mozaffari, A.; Johnson, M. R. *Org. Synth*. **1992**, *70*, 68−77.

(12) Collman, JP.; Barnes, C. E.; Woo, L. K. *Proc. Natl. Acad. Sci. U.S.A.* **1983**, *80*, 7684.

(13) Collman, J. P.; Garner, J. M.; Woo, L. K. *J. Am. Chem. Soc*. **1989**, *111*, 8141.

Table 1. ^{1}H NMR Chemical Shifts for Molybdenum and Tungsten Porphyrin Dimers

compound	H_{meso}	$H_{o'}$	$H_{m'}$	H_o	H_m	CH_2CH_3[a]	CH_2CH_3	Ar-CH_3
[Mo(OEP)]$_2$	9.20					4.32	1.78	
						3.92		
[Mo(TOEP)]$_2$	9.46	10.07	8.06	7.00	6.89	4.63/4.13	1.76	2.61
	9.29					3.09/2.88	1.44	
[W(OEP)]$_2$	8.42					4.11	1.67	
						3.76		
[W(TOEP)]$_2$	8.80	9.57	7.91	7.10	7.10	4.22/3.78	1.64	2.59
	8.50					2.95/2.63	1.29	
[(OEP)MoW(OEP)]	9.06 (Mo)					4.28/3.88 (Mo)	1.74 (Mo)	
	8.68 (W)					4.21/3.81 (W)	1.72 (W)	
[(TOEP)MoW(TOEP)]	9.41/9.19 (Mo)	9.91 (Mo)	7.95 (Mo)	6.98 (Mo)	6.98 (Mo)	4.38/3.85 (Mo)	1.65 (Mo)	2.59 (Mo)
						3.05/2.18 (Mo)	1.39 (Mo)	
	8.97/8.81 (W)	9.86 (W)	7.95 (W)	6.98 (W)	6.98 (W)	4.24/3.73 (W)	1.62 (W)	2.59 (W)
						2.95/2.69 (W)	1.36 (W)	

[a] Multiplets.

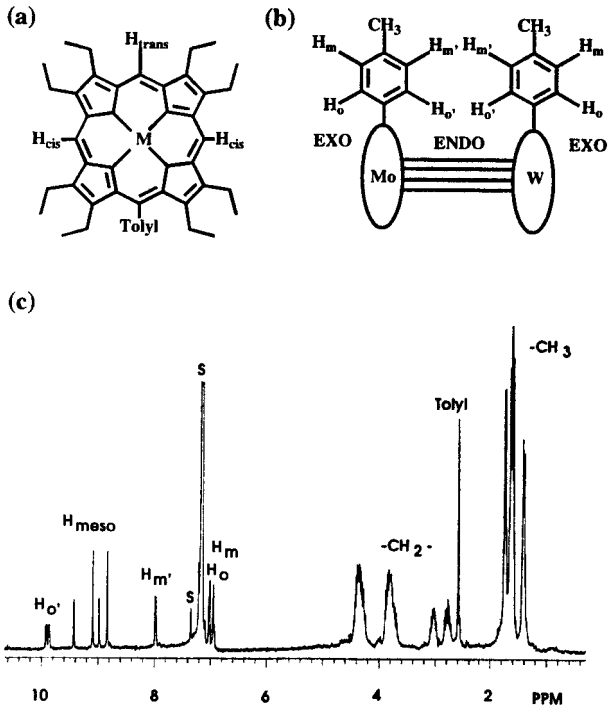

Figure 1. (a) *meso*-Proton regiochemistry in monosubstituted OEP derivatives. (b) Aryl proton regiochemistry in metalloporphyrin dimers. (c) ^{1}H NMR of **2** (C_6D_6, 20 °C).

resonances exists for each half of the heterodimer, [(TOEP)-MoW(TOEP)] (**2**). The room temperature ^{1}H NMR spectrum for **2** is shown in Figure 1.

Figure 1c also consists of bands readily assigned to the tolyl groups and the β-ethyl substituents. The *endo*-tolyl protons ($H_{o'}$ and $H_{m'}$), which are directed across the metal−metal bond, are much more strongly deshielded than the *exo*-protons (H_o and H_m). Quantitative calculations of the diamagnetic anisotropies ($\Delta\chi$) of Mo_2, W_2, and MoW quadruple bonds manifest the largest $\Delta\chi$ values yet reported, over 1 order of magnitude greater than the $\Delta\chi$ values obtained for alkynes.[15] As seen in Figure 1, the $H_{o'}$ resonances in **2** are shifted downfield by nearly 3 ppm relative to H_o.[16]

Comparison of analogous ^{1}H NMR spectra for **3** and **4** (Table 1) demonstrates that each corresponding resonance is located further downfield in the dimolybdenum species, **3**. For this reason we find it reasonable to assign the more downfield sets in **2** to the molybdenum−porphyrin half of the dimer. Nonetheless, the distinctions between Mo(TOEP) and W(TOEP) resonances are not indisputable.

Molecular models and ^{1}H NMR experiments[17] indicate that the tolyl rings in **2**, **3**, and **4** are positioned roughly perpendicular to the porphyrin plane as a result of steric interactions with the adjacent ethyl groups. The dynamic behavior of the ^{1}H NMR is not complicated by tolyl atropisomerism. A *meso*-proton of one porphyrin which is eclipsed with the opposing *meso*-tolyl group is coplanar with the tolyl protons and is thus deshielded. This deshielding is very sensitive to the angle of rotation, and is neglible when the *meso* positions are staggered ($\chi = 45°$).[10] A pronounced deshielding is only consistent with a conformation in which the *meso* positions of each porphyrin are eclipsed.

^{1}H NMR. Slow Rotation Regime. Peak broadening in the ^{1}H NMR spectrum of **2** is significant immediately upon lowering the temperature below 20 °C. Figure 2 illustrates the dynamic behavior of the *meso*- and *endo-o*-tolyl bands in **2**.

The $H_{o'}$ doublets at δ 9.81 ppm (W) and 9.86 ppm (Mo) in Figure 1 are resolved into tw separate doublets each (W, δ 9.76, 9.90 ppm; Mo, δ 9.83, 10.0 ppm) in a ratio of 0.60:0.40 at low temperature. This observation suggests that, at −70 °C, **2** exists as a 1.5:1 ratio of two conformers: the dominant conformation with $H_{o'}$ chemical shifts of δ 9.76 (W) and 9.83 (Mo) ppm, and the lesser populated conformation with chemical shifts of δ 9.90 (W) and 10.0 (Mo) ppm. The room-temperature spectrum is composed of time-averaged resonances derived from the chemical shift positions in these two conformations.

Analysis of the low-temperature *meso*-proton resonances is also consistent with the existence of two rotamers in a ratio of 1.5:1. Examination of the 2D NOESY/EXCHSY spectrum of **2** at −78 °C (Figure 3) enables a confident assignment of these two conformations as the *anti* and *gauche* eclipsed rotamers (see Figure 4). The off-diagonal resonances in the NOESY/EXCHSY spectrum of **2** may arise as a result of proton exchange between magnetically inequivalent positions or as a result of

(14) (a) Johnson, A. W.; Oldfield, D. *J. Chem. Soc., Chem. Commun.* **1966**, 794−798. (b) Bonnett, R.; Stephenson, G. F. *J. Org. Chem.* **1965**, *30*, 2791. (c) Callott, H. J.; Louati, A.; Gross, M. *Tetrahedron Lett.* **1980**, *21*, 3281. (d) Crossley, M. J.; King, L. G.; Pyke, S. M. *Tetrahedron* **1987**, *43*, 4569.

(15) (a) Chen, J. D.; Cotton, F. A.; Falvello, L. R. *J. Am. Chem. Soc.* **1990**, *112*, 1076. (b) Cotton, F. A.; James, C. A. *Inorg. Chem.* **1992**, *31*, 5298. (c) Cotton, F. A.; Eglin, J. L.; James, C. A. *Inorg. Chem.* **1993**, *32*, 681.

(16) The change in chemical shift, $\Delta\delta$, is related to $\Delta\chi$ by $\Delta\delta = (\Delta\chi/4\pi)[(1 - 3\cos^2\theta)/3r^3]$, where r is the distance of the test nucleus to the source of anisotropy and θ is the angle between the r vector and the source axis.

(17) A significant shielding of the methylene protons in the ethyl groups adjacent to the tolyl substituent is observed (δ 3.00 and 2.83 vs 4.6−3.8 ppm for **2**, Table 1), analogous to shifts in [10]paracyclophane: Agarwal, A.; Barnes, J. A.; Fletcher, J. L.; McGlinchey, M. J.; Sayer, B. G. *Can. J. Chem.* **1977**, *55*, 2575.

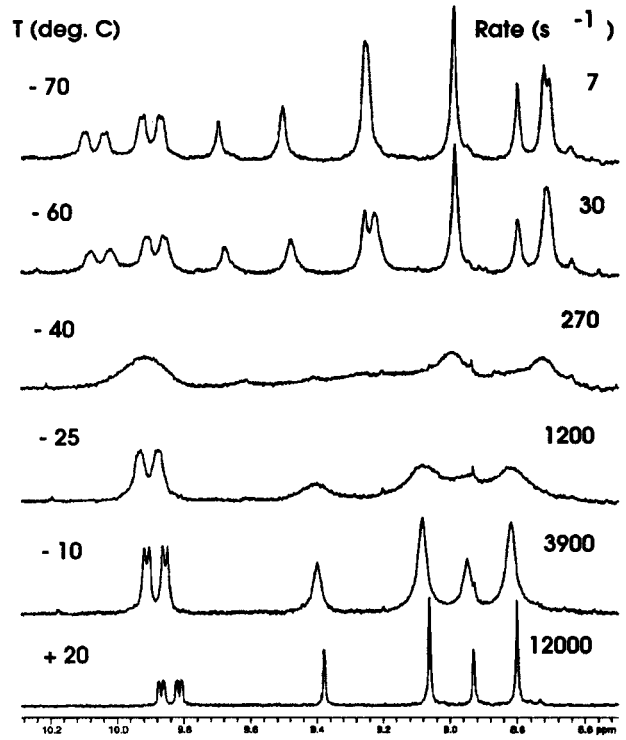

Figure 2. Variable-temperature ^{1}H NMR at 500 MHz of **2**. Rates determined by complete band shape analysis.

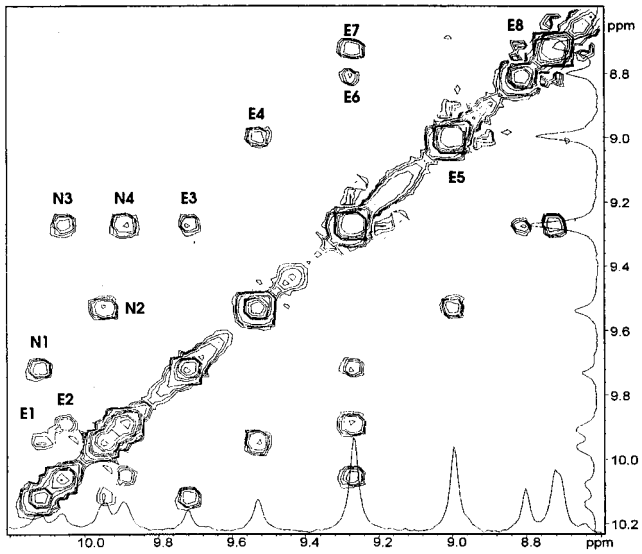

Figure 3. 500 MHz 2D NOESY/EXCHSY spectrum of **2** at −78 °C (toluene-d_8).

through-space interactions (nuclear Overhauser effect) between separate protons.[18]

There are 12 off-diagonal resonances observed in Figure 3. Of these, four (labeled N1−N4) must be a result of NOE since they relate an *endo*-tolyl $H_{o'}$ proton to a *meso*-proton. The existence of NOE cross-peaks between *endo*-tolyl $H_{o'}$ protons and *meso*-protons, but not between *endo*-tolyl $H_{o'}$ protons and β-ethyl protons, is consistent with our claim that the two low-temperature limit rotamers are eclipsed.[19] The two farthest downfield *meso*-proton resonances, at δ 9.71 and 9.52 ppm,

(18) A more complete description of the NOESY pulse sequence is available: States, D. J.; Haberkorn, R. A.; Ruben, D. J. *J. Magn. Reson.* **1982**, *48*, 286.

(19) The complete NOESY/EXCHSY spectrum is available as Supporting Information.

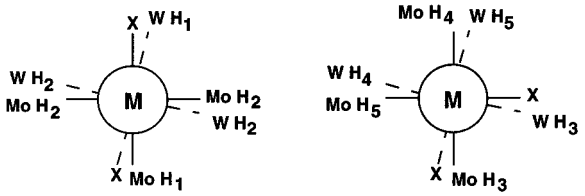

Figure 4. Eclipsed rotational isomers about a quadruple metal−metal bond showing the *meso*-proton labeling scheme used in the text. The two metalloporphyrin halves of the dimer are labeled separately for each rotamer (anti on the left, *gauche* on the right). In this work X = tolyl groups only.

are assigned as Mo H_1 and Mo H_3 according to the scheme in Figure 4. This assignment is made on the basis that Mo(porphyrin) protons should be downfield of corresponding W(porphyrin) protons (see Table 1) and protons eclipsed with the opposing tolyl substituent should be downfield of protons eclipsed with opposing *meso*-protons. The relative intensities of Mo H_1 and Mo H_3 indicate that H_1 belongs to the less populated *anti* rotamer, and H_3 to the more populated *gauche* rotamer.[20] Interestingly, W H_1 and W H_3 have slightly different chemical shifts at −60 °C (see Figure 2), but accidentally overlap in the limiting low-temperature spectrum. Nonetheless, the separate cross-peaks labeled N3 and N4 in Figure 3 identify their respective locations at δ 9.28 and 9.27 ppm.

The remaining off-diagonal resonances, labeled E1−E8 in Figure 3, may be used to identify the chemical shift positions of the remaining protons in Figure 4. As the *anti* rotamer exchanges with the gauche, Mo H_1 should exchange with Mo H_5. Figure 3 demonstrates a cross-peak (E3) which relates Mo H_1 to a third resonance buried underneath W H_1 and W H_3. Thus, the chemical shift position of Mo H_5 is determined to be δ 9.27 ppm. Likewise, Mo H_3 and Mo H_4 should become degenerate at a new chemical shift (Mo H_2) as the *gauche* rotamer returns to the anti. The NOESY/EXCHSY spectrum demonstrates an exchange peak (E4) for Mo H_3 with the resonance at δ 8.99 ppm. Because Mo H_4 and Mo H_2 are both H_{cis} and both eclipsed with *meso*-protons, they exhibit no noticeable chemical shift difference and the cross-peak relating Mo H_4 to Mo H_2 is located along the diagonal (E5).

Similar reasoning enables assignment of the five W *meso* bands. Cross-peak E6 relates W H_1 to W H_5, and cross-peak E7 relates W H_3 to W H_2. Finally, W H_4 is also exchanged with W H_2, but in contrast to Mo H_4 and Mo H_2, the tungsten protons are slightly resolved at the low-temperature limit. Nonetheless, the cross-peak relating W H_4 and W H_2, E8, is still located near the diagonal. Cross-peaks E1 and E2 are the result of $H_{o'}$ exchange between the two rotamers.

The pattern of *meso*-proton assignments at the low-temperature limit (Figure 5) is solely consistent with population of the two eclipsed rotamers as shown in Figure 4. The relative intensities of each peak are also in good agreement with the calculated values according to populations of 40% *anti* and 60% *gauche* rotamers (Table 2). Further support for the eclipsed ground-state assignments is provided by the close agreement of the observed chemical shift difference between H_1 and H_5 (Mo, 0.45 ppm; W, 0.47 ppm) and the calculated maximum deshielding expected for a tolyl group which is perfectly eclipsed with a *meso*-proton (0.47 ppm).[21] These two protons provide an ideal measure of the deshielding as both H_1 and H_5 are H_{trans},

(20) H_1 and H_3 are both eclipsed with opposing tolyl substituents; however, H_1 is trans to its own tolyl substituent and H_3 is cis. Studies[14] of similar OEP.-X porphyrin complexes indicate that H_{trans} protons are located downfield of H_{cis} protons.

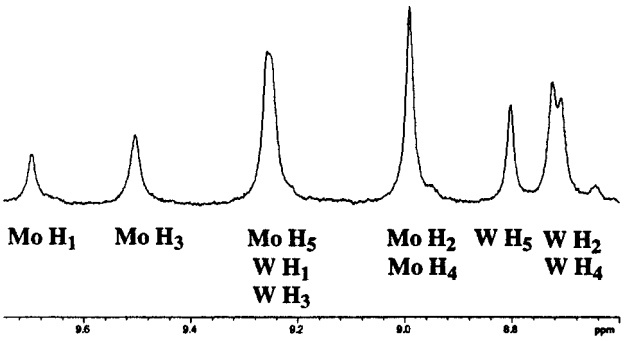

Figure 5. Assignment of the limiting low-temperature 500 MHz ^{1}H NMR spectrum of **2** according to the scheme in Figure 4.

Table 2. Calculated and Experimental Peak Integrations for the Low *T* Spectrum of **2**

chemical shift	assignment	rotamers	calculated peak integration[a]	actual peak integration
9.69	Mo H_1	*anti*	0.40	0.37
9.49	Mo H_3	*gauche*	0.60	0.52
9.24	Mo H_5	*gauche*	1.60	1.55
	W H_1	*anti*		
	W H_3	*gauche*		
8.98	Mo H_2	*2* × *anti*	1.40	1.41
	Mo H_4	*gauche*		
8.80	W H_5	*gauche*	0.60	0.52
8.70	W H_2	*2* × *anti*	1.40	1.43
	W H_4	*gauche*		

[a] *anti* = 0.40, *gauche* = 0.60, as determined from the *endo*-tolyl resonances.

but H_1 is eclipsed with the tolyl group while H_5 is not. This agreement is very good evidence in support of an eclipsed geometry between the *meso*-protons and the tolyl substituents.

The 1.5:1 ratio of *gauche:anti* eclipsed rotamers in **2** is nearly identical to the ratios previously determined for **3** and **4**.[9] Deviation from the purely statistical ratio of 2:1 is consistent with a slight thermodynamic preference (≤ 2 kcal/mol) for the *anti* conformation. In all three cases the *syn* rotamer, with tolyl substituents eclipsed, is not populated to any detectable extent. Exclusion of the *syn* rotamer is not surprising since models have shown the tolyl protons to extend across the metal−metal bond to within 0.15 Å of its center. Such an orientation would result in severe tolyl−tolyl repulsive interactions and accounts for the absence of the *syn* rotamer in all three metalloporphyrin dimers studied.

***δ*-Bond Rotational Barrier. Low-Temperature Limiting Spectrum Method.** A first estimate of the rotational barrier for **2** is possible through identification of the temperature, T_I, when line broadening of the low-temperature limiting spectrum just becomes perceptible. This method has been presented by Faller[22] as an alternative to coalescence point analysis (CPA). CPA is dependent on the chemical shift difference (Hz) between sites in the absence of exchange, and thus varies with the field strength of the spectrometer. Not only are a variety of spectrometer field strengths now in use, but the chemical shift differences between sites for *meso*-protons and *endo*-tolyl protons at the low-temperature limit are not the same. Coalescence point analysis would yield several different rotational barriers for the same molecule, and for these reasons its use is not recommended by the authors.

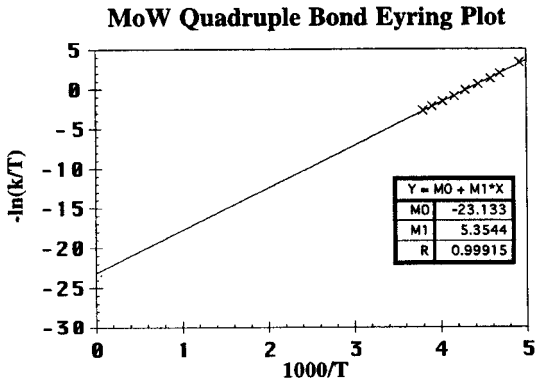

Figure 6. Eyring plot for rotation about the metal−metal bond axis in **2**.

Initial broadening of the toluene-d_8 ^{1}H NMR spectrum of **2** is seen at −80 ± 5 °C. This value of T_I results in a $\Delta G^{\ddagger}_{rot}$ = 10.7 ± 0.3 kcal/mol.[22]

Complete Band Shape Analysis. The meso, $H_{o'}$, and $H_{m'}$ protons of **2** provide eight separate spin systems (H_{cis}, H_{trans}, $H_{o'}$, and $H_{m'}$ for each metal) that may be analyzed through complete band shape analysis (CBA). As each spin system is characterized by a separate set of spectral parameters, a multiple verification of rate results from the best fit of all simulations at a given rate. The rates corresponding to each variable-temperature spectrum have been listed in Figure 2.[23] The barrier for interconversion of the *anti* and *gauche* rotamers ($\Delta G^{\ddagger}_{rot}$ = 10.6 ± 0.1 kcal/mol), determined from an Eyring plot[24] of the best-fit rates versus 1/*T* (Figure 6), is in excellent agreement with the low-temperature limiting spectrum analysis. The very low value of $\Delta S^{\ddagger}_{rot}$ renders this barrier temperature independent, within experimental error: $\Delta G^{\ddagger}_{rot} = \Delta H^{\ddagger}_{rot}$.

Vibrational Spectroscopy. The three *meso*-tolyl octaethylmetalloporphyrins (**2**, **3**, and **4**) which have been investigated by dynamic NMR[10] (vide supra) have also been characterized by resonance Raman spectroscopy. In each case enhancement of a mode assigned as the metal−metal stretch was effected with UV-excitation (363.8 nm) into the blue side of the dimer Soret band (see Figure 8). Assignment of the ν_{MM} modes was made on the basis of similar vibrational studies of other quadruply bonded group VIB dimers,[25] depolarization ratios, and subtraction of the spectrum obtained from the corresponding metalloporphyrin monomer.[26] Enhancement of the metal−metal stretch in this fashion is consistent with the enhancement mechanism which has been proposed for axial-ligand vibrational modes in resonance with the Soret band of many other metalloporphyrins. A change in the internuclear distance of the metal−metal bond could occur either via overlap of the a_{2u}

(21) *meso*-Proton deshielding due to the ring current of an aryl substituent as a function of the angle of rotation about the metal−metal bond was calculated with the Waugh−Fessenden classical model of ring current magnetic anisotropy as developed by Johnson−Bovey: Bovey, F. A. *Nuclear Magnetic Resonance*; Academic Press: New York, 1988; p 108.

(22) Faller, J. In *Encyclopedia of Inorganic Chemistry*; King, R. B., Ed., Wiley: England, 1994; pp 3914−3933.

(23) Rates were calculated with the program DNMR 5, obtained from Dr. Richard Counts at the Quantum Chemical Program Exchange, Indiana University, and adapted for use on a desktop PC. Transverse relaxation times, T_2, were obtained at each temperature from the line widths in [(OEP)-MoW(OEP)], which undergoes the same dynamic exchange but between sites which are magnetically equivalent.

(24) The formula $-\ln(k/T) = -\ln(Kk_B/h) + \Delta G^{\ddagger}/RT$ is the Eyring equation, where K is the transmission coefficient, k the rate, k_B the Boltzmann constant, and h Planck's constant. See: Sandstrom, J. *Dynamic NMR Spectroscopy*; Academic Press: New York, 1982.

(25) (a) Cotton, F. A.; Walton, R. A. *Multiple Bonds Between Metal Atoms*; Wiley: New York, 1993; pp 735−739. (b) Tait, C. D.; Garner, J. M.; Collman, J. P.; Sattelberger, A. P.; Woodruff, W. H. *J. Am. Chem. Soc.* **1989**, *111*, 9072−9077.

(26) RR spectra were also obtained for the monomers Mo(TOEP)(O) and W(TOEP)(O)(Cl). The modes assigned as ν_{MM} in the dimers were absent from the monomer spectra.

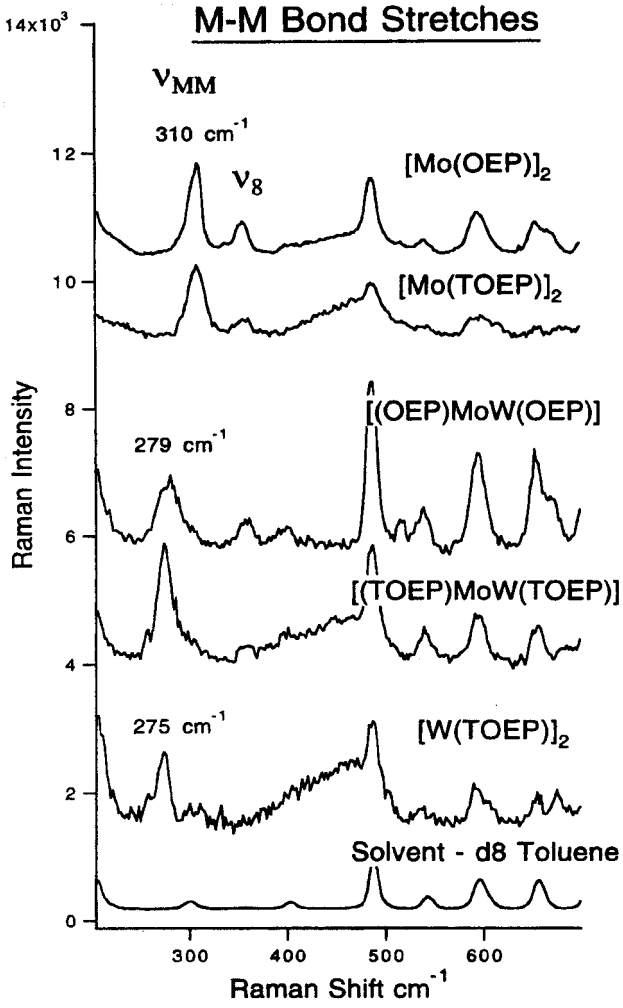

Figure 7. Low-frequency RR spectra upon excitation at 363.8 nm for **1**, **2**, **3**, **4**, and **5**. Samples were prepared in toluene-d_8 solution and flame sealed. Solvent resonances were not subtracted from the raw data, but are given for comparison. All spectra are baseline corrected. Sample stability was confirmed by ^{1}H NMR analysis following excitation.

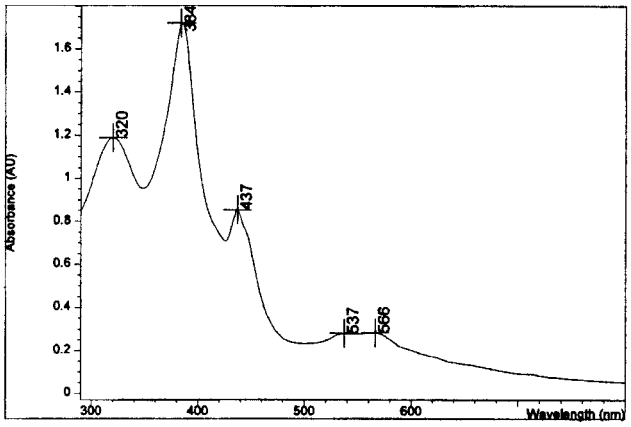

Figure 8. Absorption spectrum for **2** in benzene. All group VIB dimer electronic absorption spectra are qualitatively identical.

porphyrin orbital with the metal−metal σ-bond, or via overlap of the porphyrin $3e_g$* orbital with the metal−metal π-bonds. The change in electron density on the porphyrin that accompanies the ring-centered $\pi \rightarrow \pi^*$ Soret transition may thus result in a change in electron density and hence bond length of the metal−metal bonded axial ligand.

Table 3. Calculated Structural Parameters from Observed M−M Stretching Frequencies

	ν_{M-M}, cm^{-1}	k, mdyn/Å	D, Å[a]	bond order	ref
$[Mo(OEP)]_2$	310	2.72	2.33	4.0	this work
$[Mo(TOEP)]_2$	310	2.72	2.33	4.0	this work
[(OEP)MoW(OEP)]	279	2.89	2.30/2.40	4.0	this work
[(TOEP)MoW(TOEP)]	278	2.87	2.30/2.40	4.0	this work
$[W(OEP)]_2$	275	4.08	2.24	4.0	this work
$[Ru(OEP)]_2$	285	2.42	2.40	2.0	32
$[Ru(OEP)]_2^+$	301	2.70	2.33	2.5	32
$[Ru(OEP)]_2^{2+}$	310	2.86	2.30	3.0	32
$[Os(OEP)]_2$	233	3.04	2.37	2.0	25b
$[Os(OEP)]_2^+$	254	3.46	2.31	2.5	25b
$[Os(OEP)]_2^{2+}$	266	3.96	2.25	3.0	25b

[a] The bond lengths (D) have been estimated from an empirical relationship (ref 28), which gives distinct formulas for second and third row homodimers. Both results have been presented for the MoW heterodimers.

Table 3 summarizes the structural parameters calculated from the metal−metal bond vibrational data for several metalloporphyrin dimers. Force constants were obtained from the diatomic oscillator approximation,[27] and metal−metal distances were estimated using an empirical correlation between force constants and metal−metal bond lengths.[28]

Spectra of [(OEP)MoW(OEP)] (**1**) and $[Mo(OEP)]_2$ (**5**) were also obtained to determine the validity of the diatomic approximation wherein ligand effects (such as mass) are neglected in the calculation of metal−metal bond force constants. Figure 7 shows the low-frequency region of the RR spectra for **1**, **2**, **3**, **4**, and **5**. Our results indicate that the substantial difference in ligand mass between the OEP and TOEP porphyrin dimers has a relatively small effect on the metal−metal bond stretching frequency. The shift for the two Mo−Mo stretches is at most 1−2 cm^{-1}, and the shift for the Mo−W stretches is at most 2−3 cm^{-1}, both to lower frequency for the TOEP dimers.[29] Several other lines of evidence are also consistent with our assumption that the metal−metal stretch is essentially M_2 localized. The metal−nitrogen force constant is very weak relative to the metal−metal force constant; thus, mixing of metal−nitrogen stretching or metal−metal−nitrogen bending coordinates with the metal−metal stretch coordinates is limited. The same may not be said for analogous $M_2X_4(PR_3)_4$ dimers, since in those molecules the metal−halide force constant is comparable in magnitude with the metal−metal force constant. To estimate the exact percentage of localized diatomic character exhibited by the metal−metal stretches in $M_2(OEP)_2$ dimers, we have performed a simple normal coordinate analysis (see the Supporting Information) with the structural parameters from our single-crystal X-ray diffraction study of $[Ru(OEP)]_2$.[30] The results from this study indicate that only minor systematic corrections of a 10% or less reduction in the force constant need to be applied to the diatomic oscillator approximation used to describe metal−metal bonding between second and third row metals in porphyrin systems. These studies and the small mass

(27) $k = (3.55 \times 10^{17})\mu\nu^2$, where k = force constant (mdyn/Å), μ = reduced mass of the two metal atoms (g), and ν = vibrational frequency (cm^{-1}).

(28) Miskowski, V. M.; Dallinger, R. F.; Christoph, G. G.; Morris, D. E.; Spies, G. H.; Woodruff, W. H. *Inorg. Chem.* **1987**, *26*, 2127−2132. The appropriate equation for elements Rb−Xe is $D_{MM} = 1.83 + 1.51 \exp^{(-k/2.48)}$, where D is in Å and k is in mdyn/Å. For elements Cs−Rn, $D_{MM} = 2.01 + 1.31 \exp^{(-k/2.36)}$.

(29) Quality spectral data were not obtained for W_2OEP_2, probably due to its very poor solubility, so a third comparison is not available.

(30) Collman, J. P.; Barnes, C. E.; Swepston, P. N.; Ibers, J. A. *J. Am. Chem. Soc.* **1984**, *106*, 3500−3510.

effect seen upon substitution of TOEP for OEP provide good support for the trend observed in Table 3. The Raman data indicate that the force constants increase in the order Mo−Mo < Mo−W < W−W, implying a trend in overall metal−metal bond strength that places the heterodimer intermediate between the two homodimers, but significantly weaker than their calculated average.

In addition to the Soret, the electronic absorption spectra of **2**, **3**, and **4** exhibit an intense band at 430−440 nm (Figure 8). Although the metal−metal stretching band is strongly enhanced with excitation at 363.8 nm, it is not seen upon excitation at 432, 439, 457, 476, or 488 nm (Raman data not shown). These excitation wavelengths span the electronic transition at 438 nm and were performed to understand the scattering mechanism which gives rise to the observed metal−metal stretch. The most well-supported hypothesis is that the 438 nm band is a ligand-to-metal charge transfer from the porphyrin HOMO ($3e_g$*) to the δ^* (b_{1u}) orbital, but we have not confirmed the assignment by identification of an associated MCD *A* term.

The porphyrin skeletal vibrations observed in the frequency range 1470−1610 cm^{-1} in the *meso*-tolyl-substituted OEP dimers **2**, **3**, and **4** are similar upon excitation into either absorption band. Vibrational assignments of the porphyrin skeletal modes were inferred from the depolarization ratios and from comparisons with the vibrational spectra of Ni(OEP)[31] and $[Ru(OEP)]_2$.[32] The Ni(OEP) monomer is a very useful standard for comparison since a complete normal coordinate analysis has been correlated with the spectra,[33] and the vibrational numbering scheme for OEP vibrations was developed for this compound. The similarity of metalloporphyrin dimer spectra with metalloporphyrin monomer spectra is consistent with previous studies. The vibrational peak positions of $[Ru(OEP)]_2$ are almost identical to those in Ru(OEP)(CO),[32] and even stacked silicon phthalocyanine vibrations are not shifted significantly from the silicon phthalocyanine monomer.[34]

Figure 9 shows the high-frequency region of the RR spectra for **2**, **3**, and **4** obtained with excitation at 432 nm. The extreme complexity of these molecules has precluded us from performing complete, high-frequency region normal-mode analyses and thus being able to assign each of the observed porphyrin skeletal modes according to the scheme in ref 33. However, the overall qualitative picture which emerges upon inspection of Figure 9 demonstrates a striking similarity between the high-frequency spectra of Ni(OEP) and $[W(TOEP)]_2$. In contrast, the dimolybdenum spectrum is significantly more complicated and exhibits several distinct new features, while the molybdenum−tungsten spectrum appears as a superposition of the homodimer spectra. These features are consistent with a greater "bending-back" distortion of molybdenum−porphyrin entities, while tungsten−porphyrins resemble the four-coordinate, planar Ni(OEP). The mixed-metal dimer appears to exhibit both features simultaneously.

The ^1H NMR spectra of **2**, **3**, and **4** are also consistent with this structural difference between molybdenum− and tungsten−porphyrin complexes. The chemical shift difference of H_{cis} and H_{trans} is dominated by the through-space magnetic anisotropy of the opposing tolyl group. Assuming exchange between eclipsed ground state conformations, the magnitude of deshielding will be a simple function of distance to the tolyl group. Figure 1 clearly demonstrates that the W H_{cis} and W H_{trans} protons are much closer in their time-averaged chemical shifts than the corresponding Mo H_{cis} and Mo H_{trans}. We offer this evidence as further support of our contention that the mixed-metal dimer is simultaneously composed of one drastically distorted porphyrin (which is therefore unable to impart as large an anisotropy to the opposed W H_{cis} and W H_{trans}) and one nearly planar porphyrin (Figure 10).

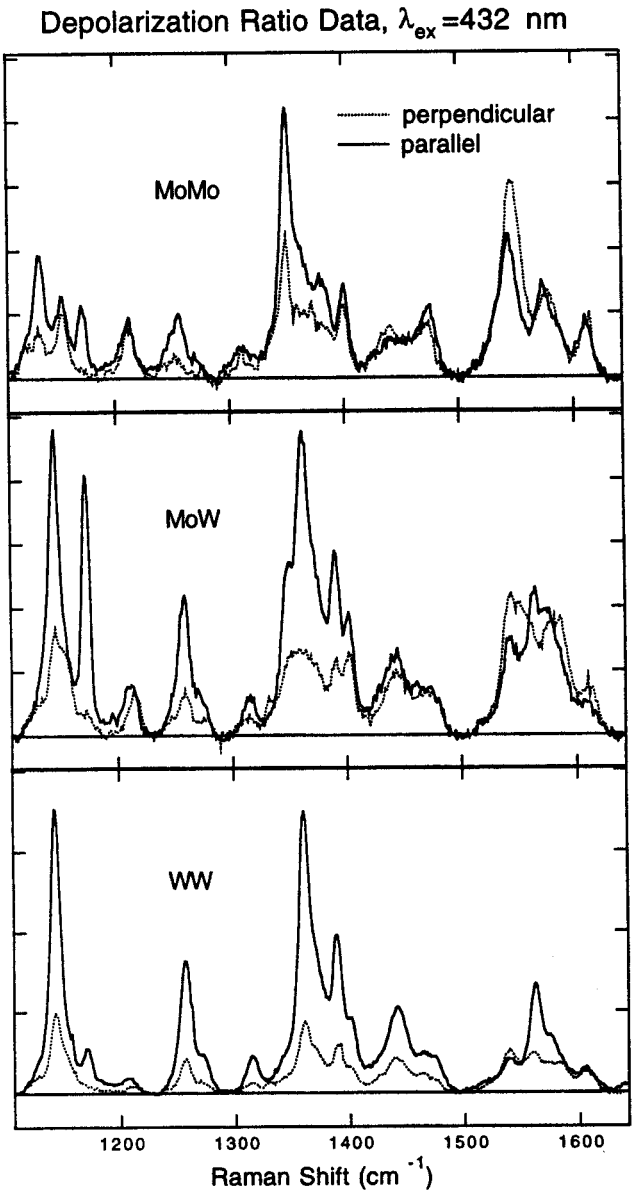

Figure 9. High-frequency RR spectra obtained for **2**, **3**, and **4** with excitation at 432 nm into an electronic charge-transfer band. Solvent was toluene-d_8 for each sample.

Discussion

We have estimated the δ-bond strengths of isostructural Mo_2,[9] W_2,[9] and MoW porphyrin dimers by measuring the barrier to rotation about the metal−metal bond. Historically, δ-bond strengths have been correlated with $\delta \rightarrow \delta^*$ electronic transition energies.[35] Such studies imply stronger δ-bond strengths for the dimolybdenum verses ditungsten quadruple

(31) Kitigawa, T.; Abe, M.; Ogoshi, H. *J. Chem. Phys.* **1978**, *69*, 4516−4525.

(32) Tait, C.Drew; Garner, J. M.; Collman, J. P.; Sattelberger, A. P.; Woodruff, W. H. *J. Am. Chem. Soc.* **1989**, *111*, 7806−7811.

(33) Abe, M.; Kitagawa, T.; Kyogoku, Y. *J. Chem. Phys.* **1978**, *69*, 4526−4534.

(34) Simic-Glavaski, B.; Tanaka, A. A.; Kenney, M. E.; Yeager, E. *J. Electroanal. Chem.* **1987**, *229*, 285−296.

(35) Cotton, F. A.; Eglin, B. H.; James, C. A. *Inorg. Chem.* **1993**, *32*, 2104−2106.

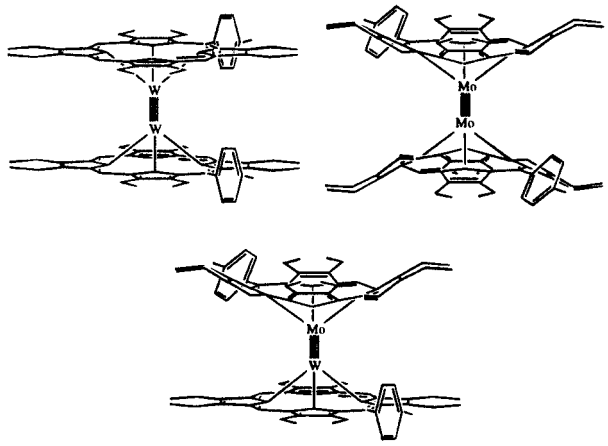

Figure 10. Structural representations of **2**, **3**, and **4** as implied by RR and ^{1}H NMR results.

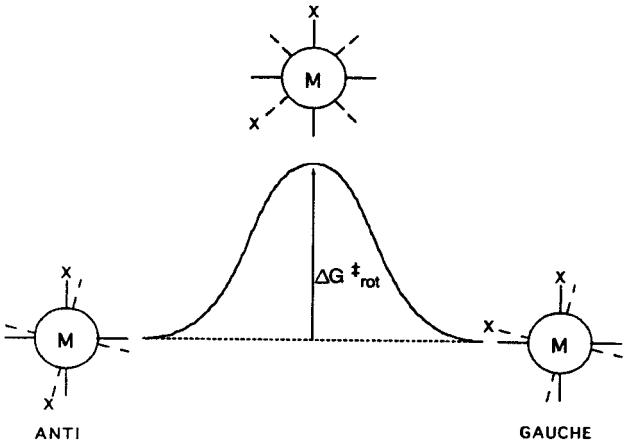

Figure 11. Definition of the δ-bond rotational barrier, $\Delta G^{\ddagger}_{rot}$, used herein.

Table 4. $\Delta G^{\ddagger}_{rot}$ in **2**, **3**, and **4** as Determined by Complete Band Shape Analysis

dimer	$\Delta G^{\ddagger}_{rot}$
[(TOEP)MoW(TOEP)]	10.6 ± 0.1
$[Mo(TOEP)]_2$	10.8 ± 0.1
$[W(TOEP)]_2$	12.9 ± 0.1

bonds,[36] in striking contrast to our results. However, recent reports[37] have indicated that several factors must be considered in the analysis of $\delta \rightarrow \delta^*$ electronic transition energies. Such factors include the amount of metal−ligand δ-bonding,[38] the degree to which configuration interaction is involved in the ground state,[39] and mixing of the $\delta \rightarrow \delta^*$ transition with metal-to-ligand charge transfer (MLCT) bands.[40] These studies conclude that simple correlations should not be made between δ-bond strength and $\delta \rightarrow \delta^*$ energies.

Measurement of the rotational barrier for quadruply bonded complexes is an accurate, direct method for estimation of the δ-bond strength. The σ and π contributions to the quadruple bond are cylindrically symmetrical, and hence exhibit no angular preferences for overlap. However, the δ-bond achieves maximum overlap in an eclipsed conformation, and is completely nonbonding when the d_{xy} orbitals are staggered at 45°. Since exchange between the *anti* and *gauche* eclipsed conformations of metalloporphyrin dimers such as **2**, **3**, and **4** requires a staggered transition state (see Figure 11), the rotational barrier, $\Delta G^{\ddagger}_{rot}$, is an accurate estimation of ΔG_{δ} in the absence of ligand steric contributions ($\Delta G^{\ddagger}_{rot} = \Delta G_{\delta} - \Delta G_s$). Previous rotational barrier studies[41] of $[Mo(OEP\text{-}X)]_2$ with linear substituents (X = formyl, isocyanate, and NH_2) all indicate a barrier to rotation which is within experimental error of that observed for $[Mo(TOEP)]_2$. Insensitivity of these rotational barriers to the incorporation of *meso*-aryl substituents allows an estimation of ΔG_s ($\leq$0.5 kcal/mol).[42]

Comparisons may now be made between the overall quadruple bond strengths for Mo_2, W_2, and MoW as well as between δ-bond strengths for the same molecules. Metal−metal quadruple bond force constants indicate that the ditungsten species, **5**, contains the strongest quadruple bond (Table 3). This result is consistent with our rotational barrier studies, which likewise suggest that the ditungsten δ-bond is also stronger than either dimolybdenum or molybdenum−tungsten (Table 4). Manning and Trogler were the first to propose that the increased radial distribution of 5d vs 4d orbitals (a consequence of relativistic effects) compensates for longer bond lengths and increased internuclear repulsions inherent to third row metal dimers.[39]

As shown in Table 3, empirical equations derived from vibrational data predict that the W_2 and Os_2 bonds are *shorter* than the metal−metal bonds in isoelectronic Mo_2 and Ru_2 congeners. Many pairs of homologous Mo_2 and W_2 dimers have been structurally characterized, including the tetraphenylporphyrin dimers ($[Mo(TPP)]_2$[43] and $[W(TPP)]_2$),[44] and in every case the W_2 bond length is about 0.10 Å *longer* than the corresponding Mo_2 bond length.[25] Although the empirical equations have proved extremely accurate with the ligand systems from which they were derived, the equations may simply not be applicable to porphyrin dimers. Calculated force constants for the W_2 and Os_2 porphyrin dimers are 25−35% larger than the corresponding values for Mo_2 and Ru_2 dimers. The magnitude of this difference is by far the largest yet observed; indeed, the ligand systems used to generate the empirical equations exhibit force constant changes of only 4−8% upon substitution from Mo−Mo to W−W.[25] However, most of these ligand systems bridge the metal−metal bond, and thus may be expected to greatly affect the strength of the metal−metal bond through their own steric restraints and electronic preferences. The large dependence of force constant on metal identity in our systems may well be a result of the unbridged, *unrestrained* nature of the metal−metal bond. That the metal−metal stretches in metalloporphyrin dimers are essentially M_2 localized is also supported by a detailed analysis given as Supporting Information. Normal-mode calculations therein indicate that the contribution of metal−metal motion to the potential energy distribution (PED) of the vibrations assigned

(36) Cotton, F. A.; Extine, M. W.; Felthouse, T. R.; Kolthammer, B. W. S.; Lay, D. G. *J. Am. Chem. Soc.* **1981**, *103*, 4040−4045.
(37) Hopkins, M. D.; Gray, H. B.; Miskowski, V. M. *Polyhedron* **1987**, *6*, 705−714.
(38) Sattelberger, A. P.; Fackler, J. P. *J. Am. Chem. Soc.* **1977**, *99*, 1258−1259.
(39) Manning, M. C.; Trogler, W. C. *J. Am. Chem. Soc.* **1983**, *105*, 5311−5320.
(40) Hopkins, M. D.; Schaefer, W. P.; Bronikowski, M. J.; Woodruff, W. H.; Miskowski, V. M.; Dallinger, R. F.; Gray, H. B. *J. Am. Chem. Soc.* **1987**, *109*, 408−416.
(41) Collman, J. P.; Woo, L. K. *Proc. Natl. Acad. Sci. U.S.A.* **1984**, *81*, 2592−2596.
(42) The steric component of the barrier must be less than the difference in measured barriers of OEP-X derivatives. These barriers are conveniently tabulated in ref 41.
(43) For $[Mo(TPP)]_2$, the Mo−Mo separation is 2.24 Å: Yang, C.-H.; Dzugan, S.; Goedken, V. L. *J. Chem. Soc., Chem. Commun.* **1986**, 1313−1315.
(44) For $[W(TPP)]_2$, the W-W separation is 2.33 Å: Kim, J. C.; Goedken, V. L.; Lee, B. M. *Polyhedron* **1996**, *15*, 57−62.

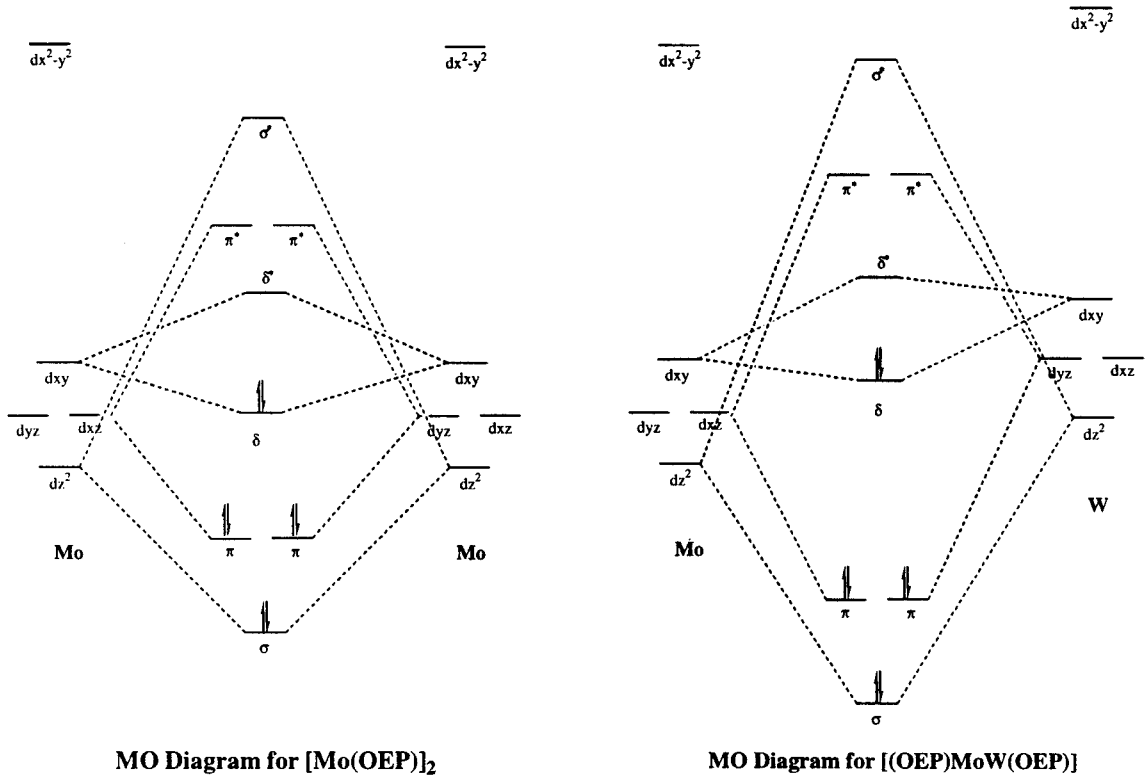

MO Diagram for $[Mo(OEP)]_2$ **MO Diagram for [(OEP)MoW(OEP)]**

Figure 12. MO diagrams for homonuclear and heteronuclear metal−metal quadruple bonds.

as ν_{MM} are on the order of 80−90%. The nearly complete isolation of the metal−metal stretch in these molecules may be understood as a consequence of the relatively large mass of the metal atoms, relatively strong metal−metal bond, and relatively weak metal−porphyrin stretching and bending interactions.

Despite the preponderance of evidence suggesting that third row metals form significantly stronger bonds than second row metals, in neither the rotational barrier nor the vibrational studies is the dimolybdenum bond significantly strengthened by substitution of a single tungsten atom. Table 3 manifests a small increase in quadruple bond strength for MoW relative to the Mo_2 species; however, Table 4 demonstrates the presence of a slightly *weaker* MoW δ-bond.

Molecular orbital theory predicts that the bond strength, ΔE, of a metal−metal bond will be dominated by two factors. The interaction energy will be made larger as the atomic orbitals achieve more geometric overlap via incorporation of more diffuse orbitals. However, ΔE is a maximum when the initial energies of the interacting orbitals are identical. Previous heterodimer studies[8] have not directly addressed how the strength of a heterodimeric metal−metal bond is affected by the difference in atomic orbital energy levels. Greater electronegativity of Mo^{II} relative to W^{II} lowers the energy levels of its atomic d-orbitals (Figure 12). Molecular orbital theory predicts that mismatch of the atomic orbital energies will have a deleterious effect on the interaction energy for formation of the heteronuclear bond.

The face-to-face nature of $d_{xy}-d_{xy}$ overlap does not make effective use of the radially diffuse third row d_{xy} orbital. Thus, the MoW δ-bond is slightly weakened from the homonuclear Mo_2 congener upon incorporation of the lower energy W $5d_{xy}$ orbital. This slight weakening occurs despite the increased radial distribution of the 5d d_{xy} orbital. In contrast, the σ- and π-bonds are composed of atomic d-orbitals which have their distribution maxima directed toward each other, as opposed to the face-to-face orientation required for δ-bond formation. Direct orientation of the d_{z^2} and d_{xz}, d_{yz} orbitals enables a more efficient utilization of the more diffuse 5d orbitals for σ- and π-bonding, hence, the force constant[45] for the overall quadruple bond in MoW is increased from its value in Mo_2. The same result is seen in the resonance Raman studies of $MoW(Cl)_4(PMe_3)_4$ and $Mo_2(Cl)_4(PMe_3)_4$.[7]

Repeated attempts to obtain X-ray suitable single crystals of the quadruple bonded metalloporphyrin dimers have been unsuccessful. Such a study may be expected to reveal a bond length for MoW which is slightly increased from the average lengths of Mo_2 and W_2. Although not available for the porphyrin dimers, Morris has reported the crystal structure for $MoW(Cl)_4(PMe_3)_4$[7] and Cotton has determined analogous structures of $Mo_2(Cl)_4(PMe_3)_4$[46] and $W_2(Cl)_4(PMe_3)_4$.[46] The M−M bond distances increase in the order Mo_2 (2.130 (0) Å) < MoW (2.2092 (7) Å) < W_2 (2.262 (1) Å). Indeed, the MoW bond length is approximately 0.015 Å longer than the average of the homodimers, consistent with our comparison of the three ν_{MM} force constants for **2**, **3**, and **4**.

Conclusions

The rotational barrier ($\Delta G^{\ddagger}_{rot} = 10.6 \pm 0.1$ kcal/mol) and metal−metal bond force constant ($k = 2.87$ mdyn/Å) have been reported for the mixed-metal dimer [(TOEP)MoW(TOEP)]. The results indicate the existence of competing effects on the determination of heterometallic bond strengths. Atomic orbital energy mismatch due to a difference in metal atom electronegativities causes a net loss of Mo d_{xy}−W d_{xy} interaction energy

(45) Estimates indicate that the δ-bond contributes only about 10% of the overall bond strength; therefore, trends in the quadruple bond force constants will be primarily indicative of changes in the σ- and π-bond strengths.

(46) Cotton, F. A.; Extine, M. W.; Felthouse, T. R.; Kolthammer, B. W.; Lay, D. G. *J. Am. Chem. Soc.* **1981**, *103*, 4040.

and thus a δ-bond which is slightly weaker in MoW than in either Mo_2 or W_2. However, the incorporation of radially diffuse W 5d orbitals increases the geometric overlap between the respective Mo and W d_{z^2} and d_{xz}, d_{yz} orbitals which form heterometallic σ- and π-bonds. The result is a metal−metal bond force constant which is slightly higher for MoW than Mo_2, but still weaker than the average of Mo_2 and W_2. We now propose that the unbridged heteronuclear MoW quadruple bond does not exhibit bonding which may simply be described as an average of that observed in the homodimers. Our results indicate that heteronuclear metal−metal bonds are slightly weaker than the average of the homodimers due to a decrease in effective orbital mixing resulting from the difference in constituent atomic orbital energies.

Acknowledgment. We thank the NSF (Grant CHE 9123187-A4) for financial support. Special thanks to the mass spectroscopy facility at UCSF and Dr. Doris Hung at Northwestern for mass spectra of **1** and **2** and to Pharmacyclics for their generous gift of diethylpyrrole used in the syntheses of H_2OEP and H_2-TOEP.

Supporting Information Available: Complete 2D NOESY/EXCHSY spectrum, calculated and experimental mass spectra for (OEP)MoW(OEP)PF_6 and (TOEP)MoW(TOEP), and normal coordinate analyses for M_2(porphyrin)$_2$ dimers (56 pages). See any current masthead page for ordering information and Web access instructions.

JA972130M